Materials Chemistry and Physics 122 (2010) 305–310

Contents lists available at ScienceDirect

Materials Chemistry and Physics

journal homepage: www.elsevier.com/locate/matchemphys

Chemical solution deposited lanthanum zirconium oxide thin films: Synthesis and chemistry

H.S. Chen*, R.V. Kumar, B.A. Glowacki

Department of Materials Science and Metallurgy, University of Cambridge, Pembroke Street, Cambridge CB2 3QZ, UK

ARTICLE INFO

Article history:
Received 31 August 2009
Received in revised form 26 January 2010
Accepted 19 February 2010

Keywords:
Superconductors
Crystal growth
Sol–gel growth

ABSTRACT

Pyrochlore lanthanum zirconium oxide (LZO) thin films textured along ⟨4 0 0⟩ are synthesized using lanthanum acetate hydrate, zirconium propoxide, propionic acid, acetic acid glacial, and methanol as precursors. The materials growth and chemistry are investigated by X-ray diffraction (XRD), scanning electron microscopy (SEM), Fourier transform infrared spectroscopy (FTIR), and thermal gravimetric analysis (TGA). The formation of inkjet printed LZO films on Ni-5%W tape is found to be based on the decomposition of the LZO precursor solution. In the annealing process, Zr metal–oxides bonds are first eliminated between 150 and 250 °C, while carboxylates from precursors remain in LZO after the annealing carried out at 900 °C for an hour. Annealed LZO films have dense and smooth structure that are composed of nanoparticles sizing 10–15 nm and some pinholes sizing 25–35 nm accounted for less than 0.1% of the area are observed.

1. Introduction

Lanthanum zirconium oxide ($La_2Zr_2O_7$ or LZO) is a well-known pyrochlore material and is considered of interest in high dielectric constant application in the Si-based industry, thermal barriers, radiation resistant layer, and buffer layers for YBCO-based superconductors [1–10]. Various synthetic methods have been reported to prepare LZO films in the past decade. Solid state reaction is often utilized to synthesize LZO films, for example, Lian et al. obtained pyrochlore $(La_{1-x}Ce_x)_2Zr_2O_7$ ($x = 0$, 0.1, 0.2) films by sintering a mixture of ZrO_2, CeO_2 and LaO_3 powders at 1500 °C for 32 h [11]. Vacuum depositions are also widely employed to prepare LZO films. Chiodelli and Scagliotti synthesized LZO films by the e-beam technique followed by a post sintering process [5]. Solution-processed LZO materials have advantages of simplicity of process, low cost, and capability of mass production. In 1990, Kido and Komarneni successfully prepared LZO via a sol–gel route using metal acetylacetonates as precursors [6]. In 1998, Ota et al. synthesized Y_2O_3-substituted $La_2Zr_2O_7$ by the hydrazine method using zirconium chloride, lanthanum chloride, yttrium chloride, and hydrazine monohydrate as starting materials [12].

Solution-based LZO films have drawn much attention in applications of superconductors [13]. The pseudocubic lattice parameter of the pyrochlore LZO is 3.81 Å that provides a small lattice mismatch of only 0.5% and 1.8% for *a*- and *b*-axis of YBCO ($a = 3.83$ Å and $b = 3.88$ Å), respectively, so LZO film have been considered a suitable buffer layer for YBCO coated conductors [3,10]. In 2000, researchers in Oak Ridge National Laboratory established that LZO films with a high degree of a biaxial texture can be successfully obtained on textured cubic Ni (1 0 0) substrates (lattice parameter ~3.52 Å) via the sol–gel route along with a post annealing process [8–9]. In addition, a non-sol–gel or so-called chemical solution deposition method using lanthanum pentanedionate and zirconium pentanedionate dissolving in propionic acid as precursors was also presented [10]. Preparation of biaxial LZO films by wet chemical approaches, either sol–gel or chemical solution deposition methods, generally involves three stages: synthesis of precursors, coating of precursors on a textured substrate, and annealing process. It has been known that annealing and coating parameters strongly affect the microstructure of LZO films. For example, densification and porosity of the LZO films after annealing process increase and decrease respectively as the coating rate of LZO precursors on Ni substrate is increased [3,10]. For synthetic process of precursors, however, chemistry of precursor is often ignored in films processing. Precursor viscosity and composition can dominate morphology and chemical composition of wet films, and thus influences the growth of LZO films.

Processing of LZO thin films in sol–gel and chemical solution deposition methods are very similar. But the chemistry of precursors is quite different. A precursor (sol) from sol–gel is a suspension containing solid nanoparticles, while a precursor (solution) from the chemical solution deposition method is a solution containing solvated molecules. This difference in the basic nature of the two systems likely leads to a difference in the mechanism of film

* Corresponding author. Tel.: +44 1223 334315; fax: +44 1223 334567.
E-mail address: sean.chen@cantab.net (H.S. Chen).

0254-0584/$ – see front matter.
doi:10.1016/j.matchemphys.2010.02.028

growth. The procedures of wet chemical synthesis are relatively straightforward, but understanding the fundamentals involved in precursor synthesis, coating process, along with subsequent heat treatment are complicated. Few studies about the materials chemistry and growth are reported. In this paper, we report on a wet chemical method to synthesize LZO film and examine the chemistry during the materials growth.

2. Experimental

2.1. Materials

Lanthanum acetate hydrate powder, $La(CH_3COO)_3{\cdot}xH_2O$ (99.9%, Aldrich) was first dried at 170 °C for an hour. Zirconium (IV) propoxide, $Zr(OCH_2C_2H_5)_4$ in 1-propanol (70 wt.%, Aldrich), propionic acid, C_2H_5COOH (99.5%, Fluka-Garantie), acetic acid glacial, CH_3COOH (analytical reagent grade, Fisher), and methanol anhydrous, CH_3OH (99+%, Aldrich) all as liquids were used as received. LZO was prepared in a stoichiometric ratio. Lanthanum solution was first prepared by dissolving the 8 mmol dried lanthanum acetate in 34 mmol propionic acid at 80 °C (~50.1 wt.%). The solution was cooled to room temperature after it transformed to a clear liquid. Zirconium solution was prepared by rapidly mixing 8 mmol zirconium propoxide with 16 mmol glacial acetic acid at room temperature (~55.7 wt.%). A LZO precursor solution was obtained by dilution of a mixture of the above zirconium and the lanthanum solutions with methanol to a concentration of 0.2 mol kg^{-1}.

2.2. Coating process and heat treatment

A piece of highly textured Ni-5%W 50 μm thick substrate manufactured for the purpose of the superconducting was cleaned sequentially by ethanol followed by acetone in an ultrasonic system along with a thermal treatment at 850 °C to remove organics and then was placed 30 mm below the nozzle of a inkjet printer [13–15]. A computer-controlled electronic system was used to allow the nozzle open for a fixed time period so that a set amount of ink could be deposited. Nozzle opening time and inter-drop distance were set 500 μs and 4 mm, respectively. LZO precursor solution films were printed as a 5 mm × 25 mm track on the textured Ni substrates of 5 mm × 40 mm at room temperature under ambient atmosphere, as shown in Fig. 1. The LZO precursor solution used in the inkjet printer concentration was 0.05 mol kg^{-1}. The as-deposited sample was then moved to a pre-purged furnace. The annealing temperature, heating rate, and duration of time, and atmosphere are 900 °C, 10 °C min^{-1}, 1 h, and Ar-5%-H_2, respectively.

2.3. Characterizations

A change in sample weight as a function of temperature was examined by thermogravimetry analysis (TGA, TA Instruments Q500) with a heating rate of 5 °C min^{-1} from room temperature to 1000 °C in air. The chemical composition of sample powders or liquids was directly analyzed by Fourier transform infrared (FTIR, Bruker Optics Tensor 27 FT-IR) spectrometer. X-ray diffractometer (Philiips PW 1830/00 with Cu K radiation) was employed to study the crystallography in 2θ-scan mode. The out-of-plane orientation was judged by estimating the full width at half maximum (FWHM) of diffraction peaks obtained from ω-scan mode at fixed 2θ with 1/12° of diversion slit (i.e. rocking curve at omega). The surface morphology was investigated by field emission electron scanning microscope (FEGSEM, JEOL 6340F).

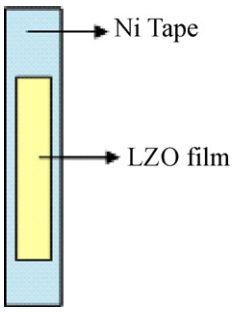

Fig. 1. The LZO film is printed as a 5 mm × 25 mm track on a Ni-5%W substrate of 5 mm × 40 mm.

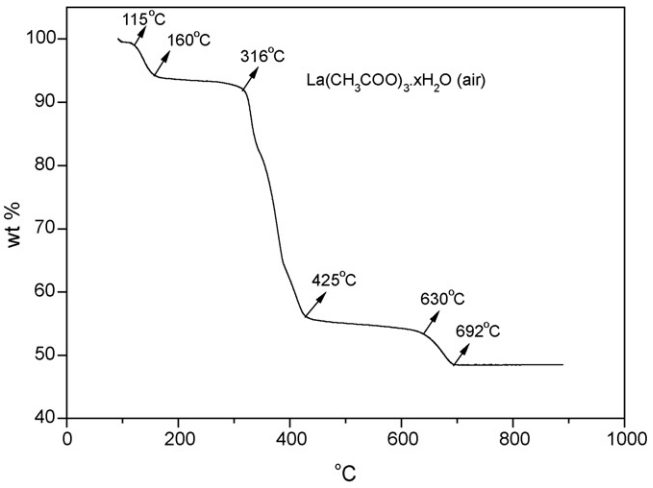

Fig. 2. TGA of lanthanum acetate hydrate burned in the atmosphere.

3. Results and discussion

3.1. Characterizations of chemicals

Weight loss of $La(CH_3COO)_3{\cdot}xH_2O$ is shown in Fig. 2. The first drop at 115–160 °C is assigned to the evaporation of water via dehydroxylation in lanthanum acetate hydrate, indicating water could be removed from the hydrate at around 160 °C. The weight ratio of water in the hydrate measured from the TGA curve was 6.2%, so the lanthanum acetate hydrate is rewritten as $La(CH_3COO)_3{\cdot}1.16H_2O$. The second drop from 316 to 425 °C may be attributable to a pyrolysis that may result in soot decomposition or combustion of $La(CH_3COO)_3$ due to the removal of organics. The final weight loss from 630 to 692 °C is thought to be the removal of carbon soot that may oxidize to carbon monoxide or dioxide, depending upon the rate of heating and the availability of oxygen. In addition, two minor weight losses in the TGA curve are considered an unstable heat flow in the initial stage (below 100 °C) and a non-uniform volume loss of a stack of dried particles in the temperature region (354–386 °C).

Fig. 3 displays FTIR spectra of the lanthanum acetate hydrate and the zirconium propoxide. A broad band at around 3220 cm^{-1} resulted by H_2O in the lanthanum acetate hydrate, as shown in Fig. 3. The O–C=O of $La(CH_3COO)_3$ appears at 539–665 and 1403–1541 cm^{-1} [16]. The peaks at 1054 and 944 cm^{-1} are caused

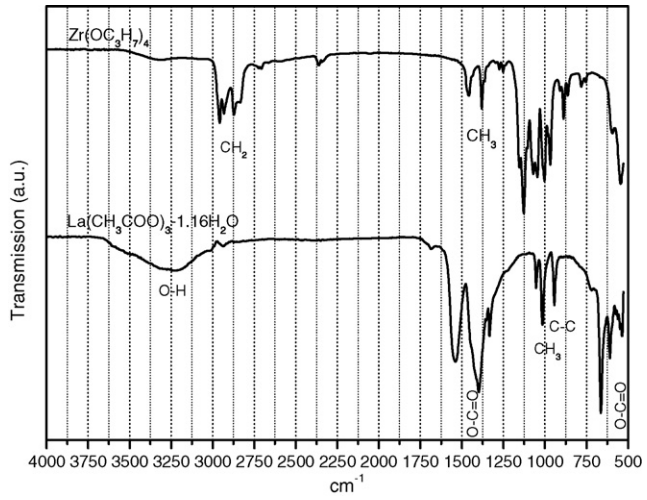

Fig. 3. FTIR spectra of lanthanum acetate hydrate and zirconium propoxide.

by CH_3 and C–C of $La(CH_3COO)_3$. For zirconium propoxide, the peaks in the ranges of 2831–2963 cm^{-1} and 1379–1460 cm^{-1} are caused by the stretching and the vibration modes of the CH_2 and CH_3 bonding of the zirconium propoxide, respectively. The peaks at around 1039–1125 cm^{-1} are attributed to the Zr–O–C vibrations.

3.2. Preparation of LZO precursor solution

LZO precursor solution is prepared by mixing a lanthanum solution with a zirconium solution and diluted by methanol to decrease the viscosity of ink for inkjet printing. Lanthanum acetate hydrate needs to be dried at 170 °C for an hour according to the TGA data to ensure a complete elimination of water that may degrade a Zr precursor. In order to dissolve $La(CH_3COO)_3$ that is expected to dissolve in some organic acids such as acetic or propionic acids, we first tried acetic acids but it did not show a sufficient solubility for dried lanthanum acetate $La(CH_3COO)_3$. So propionic acid is used instead in the present study. $La(CH_3COO)_3$ dissolves well in the propionic acid at 80 °C and forms a clear solution at 80 °C (but also at room temperature). The La solution in an equilibration is expected to contain not only ions of La^{+3}, CH_3COO^-, $C_2H_5COO^-$, H^+, but also complexes composed of La^{+3}, CH_3COO^-, and $C_2H_5COO^-$, as both the acetate and the propionate anions may coordinate to the La cation. The chemical equation of the formation of La solution is simply shown below.

La solution

$$La(CH_3COO)_3 + C_2H_5COOH \overset{80^\circ C}{\longleftrightarrow} La^{3+} + 3CH_3COO^- + C_2H_5COO^- + H^+ \quad (1)$$

On the other hand, zirconium propoxide can easily absorb water in atmosphere leading to rapid hydrolysis and degradation of metal–oxide bonds. As shown in Fig. 4, absorptions between 1039 and 1125 cm^{-1} corresponding to Zr–O–C bonds dramatically decreases as the zirconium alkoxide ages in air for 15 min. To avoid this degradation, some stabilizers must be introduced into zirconium propoxide. Acetic acid, which is usually used to modify metal alkoxides in a sol–gel process and can dissolve zirconium propoxide appropriately, is used as a stabilizer in the present study. Without an acetic acid stabilizer, zirconium propoxide degrades in seconds and forms a white precipitate in the atmosphere. A metal–oxide molecule is able to react with acetic acid and produce a metal alkoxo–acetate complex, so $Zr(OC_3H_7)_x(CH_3COO)_y$ complexes are expected to form in the Zr solution. Note that the commercial zirconium propoxide is preserved in an alcohol which may affect the chemistry of the Zr solution. In a chemical reaction, for example sol–gel process, alcohols chemically interact with metal alkoxides at the molecular level via the alcoholysis that may affect a reaction process [17]. The alcoholysis will result in the formation of a chain molecule based on the alkoxide [18].

$$M(OR_1)_n + xR_2OH \leftrightarrow M(OR_1)_{n-x}(OR_2)_x + xR_1OH \quad (2)$$

In the present case, 1-propanol is used as medium for zirconium propoxide so it would not significantly change the zirconium propoxide as $Zr(OC_3H_7)_{4-x}(OC_3H_7)_x$ is just $Zr(OC_3H_7)_4$. Addition of acetic acid into zirconium propoxide/1-propanol is represented in the following equation.

Zr solution

$$Zr(OC_3H_7)_4 + C_3H_7OH + CH_3COOH \overset{R.T.}{\longleftrightarrow} Zr(OC_3H_7)_4 + Zr(OC_3H_7)_x(CH_3COO)_y + C_3H_7OH + CH_3COOH \quad (3)$$

where coefficients are not balanced. After mixing the Zr solution with the La solution, followed by a dilution of methanol, a clear mixture is obtained. The mixture was found to keep stable for several months. Fig. 5 (curve a, b, and c) gives the FTIR spectra of the mixture along with zirconium propoxide and lanthanum acetate hydrate for reference. The spectrum of the mixture displays mixed characteristics of the zirconium propoxide and the lanthanum acetate, as shown in curve c in Fig. 5. The O–H and C–O single stretch bond of alcohols appear at 3200–3500 and 1025 cm^{-1}, respectively. Moreover, the C–H stretch from zirconium propoxide shows up at 2826 and 2948 cm^{-1} that is broadened by the C–H stretch of alcohols and $La(CH_3COO)_3$ near 3000 cm^{-1} in curve c. The absorptions at 1039–1125 cm^{-1} and 1403–1541 cm^{-1} corresponding to Zr–O–C and O–C=O of the carboxylates in the mixture respectively suggest that there is no significant change in La and Zr compounds, implying that the mixture is a solution rather than sol. So the mixing process of the La and the Zr solutions toward the LZO precursor solution can be described by the following equation.

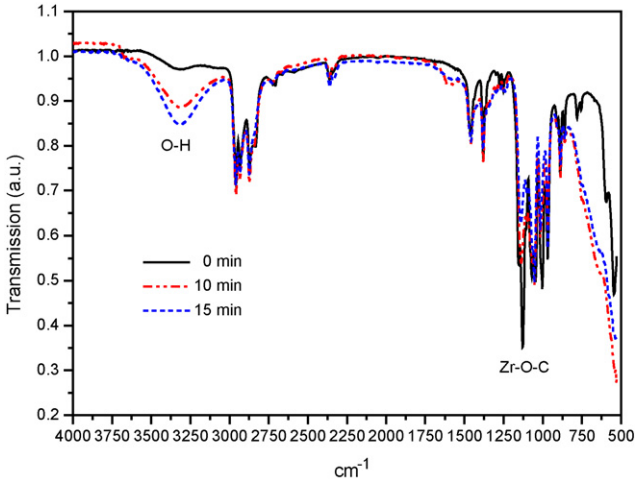

Fig. 4. FTIR spectra of $Zr(OC_3H_7)_4$ aged in the air for 10 and 15 min. It shows that the absorption between 3000 and 3400 cm^{-1} relating to H_2O readily increases with decrease in the absorption between 1125 and 1039 cm^{-1} corresponding to Zr–O–C bonding. The absorption between 500 and 800 cm^{-1} corresponds to ZrO_2.

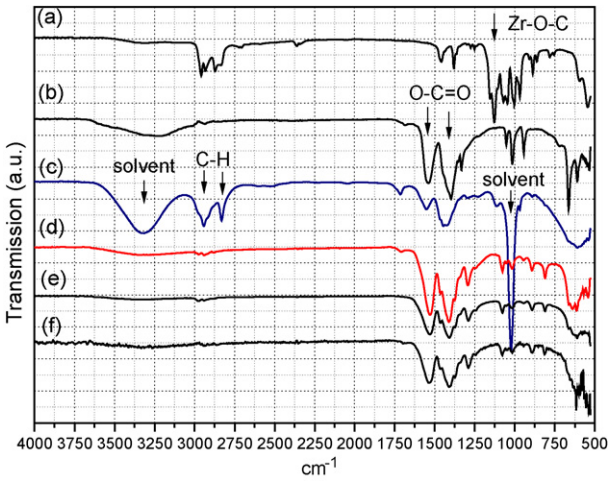

Fig. 5. FTIR spectra of $Zr(OC_3H_7)_4$ (a), $La(CH_3COO)_3$ (b), as-prepared LZO precursor solution (c), LZO precursor film dried overnight at room temperature (d), LZO film dried at 150 °C for an hour (e), LZO film dried at 150 °C for an hour followed by 250 °C for another hour (f).

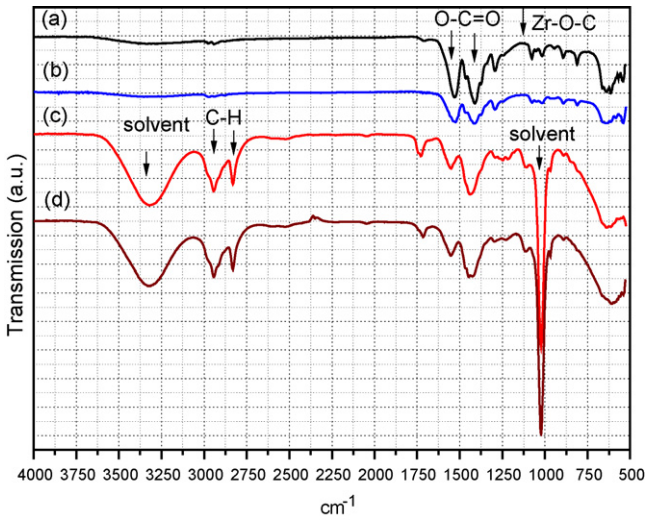

Fig. 6. FTIR spectra of the LZO precursor solution aged in the atmosphere for 3 months: LZO precursor film dried overnight at room temperature (a), precipitates of aged LZO precursor solution (b), upper liquid of aged LZO precursor solution (c), and as-prepared LZO precursor solution (d).

LZO solution

$$\mathrm{La(CH_3COO)_3 + C_2H_5COOH + Zr(OC_3H_7)_4 + C_3H_7OH + CH_3COOH + CH_3OH \leftrightarrow La(CH_3COO)_m(C_2H_5COO)_n + Zr(OC_3H_7)_4 + Zr(OC_3H_7)_x(CH_3COO)_y + C_2H_5COOH + C_3H_7OH + CH_3COOH + CH_3OH} \quad (4)$$

where coefficients are not balanced. Quantitative study has not been carried out in this study yet and it is necessary to identify the exact composition of the complexes.

3.3. Aging effect

When a LZO precursor solution was aged for three months, some white precipitates were found in the solution. FTIR spectra of the upper liquid and the precipitates are nearly identical to those of an as-prepared LZO precursor solution and a LZO precursor film dried at room temperature respectively, as shown in Fig. 6. Note that the Zr–O–C (1039–1125 cm^{-1} in curve b) absorbance of the precipitates less than that in the precursor film, which implies that Zr–O–C bonds degrades and might be related to the precipitation of solution. Indeed, zirconium alkoxides are less stable than lanthanum acetate so that alkoxides easily turns into metal–oxides due to the break of metal–oxide bonds. The degradation of the aged LZO precursor solution is expected as there is no intrinsic change in the Zr compounds after the Zr solution mixing with the La solution as shown in Eq. (4). Fig. 7 (curve c) indicates the precipitates have some crystallinity, however, it is unable to connect the diffraction peaks to crystallographic data of La or Zr-related crystals and their mixtures. The degradation of Zr–O–C usually accompanies formation of metal–oxides. But there is no zirconium oxide-related peaks identified. The precipitates are thought to be a mixture of some complexes composed of several compounds used in this study. The Zr–O–C bonds are still present in the LZO precursor film dried at room temperature over night, which displays an amorphous structure, as shown in Fig. 6 (curve a) and Fig. 7 (curve b). The above results show that the decomposition of the Zr–O–C bonds may lead to precipitates but there is no direct evidence that the decomposition causes the crystallinity.

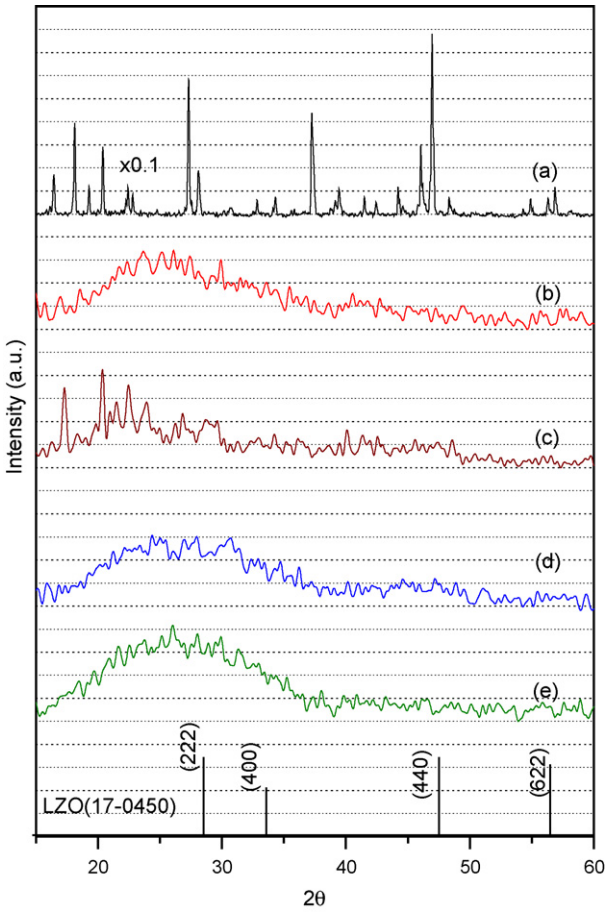

Fig. 7. XRD patterns of lanthanum acetates (a), LZO precursor film dried at room temperature (b), precipitates of aged LZO precursor solution (c), LZO precursor films dried at 150 °C for an hour (d), and 150 °C for an hour followed by 250 °C for another hour (e).

3.4. Annealing at low temperature

The LZO precursor solution and LZO precursor solution film dried at room temperature involve zirconium metal–oxide and carboxylate bonds as confirmed by FTIR spectra, as shown in Fig. 5 (curves c and d). A sample treated at 150 °C for an hour also shows a similar result, as shown in Fig. 5 (curve e). Besides solvent absorption, the composition of the dried films at both 150 °C and room temperature is similar to that of the LZO precursor solution. But when the sample is further treated at 250 °C for another hour, the C–H and Zr–O–C absorptions at the ranges of 2831–2963 cm^{-1} and 1039–1125 cm^{-1} decrease, however, O–C=O are still present in the sample, as shown in Fig. 5 (curve f). This event shows that zirconium propoxide first composes before acetates are removed. Since there is no zirconium oxides-related diffraction peaks observed in XRD analysis (curve e in Fig. 7), zirconium ions are suggested to be bonded instead by carboxylate anions, e.g. acetate anions that are strong ligands to metal ions [19]. Presumably, this reaction is the cause of the gel formation in the annealing process. This presumption may be supported by the XRD data in Fig. 7 (curve d and e), which indicates that the sample structure become more amorphous when annealed at 250 °C, implying the formation of gel. Taken the results together, the precursor solution is considered to transform to hybrid organic–inorganic compounds or gel phase consisting of lanthanum, zirconium, and carboxylates at 250 °C. Accordingly, the subsequent film nucleation and growth process would be based on the compounding/crystallization of lanthanum and zirconium ions in the gel phase while organic compounds gradually removed

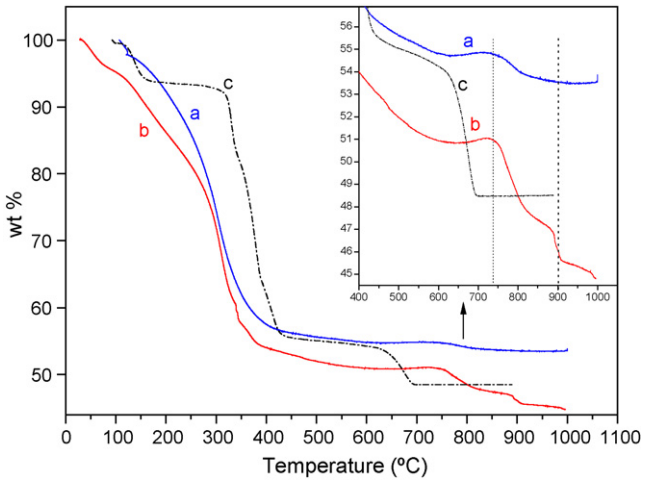

Fig. 8. TGA data of the LZO precursor solution (a) and film dried overnight at room temperature (b). Curve c is $La(CH_3COO)_3 \cdot 1.16H_2O$. The inset shows the weight change in the range 400–1000 °C.

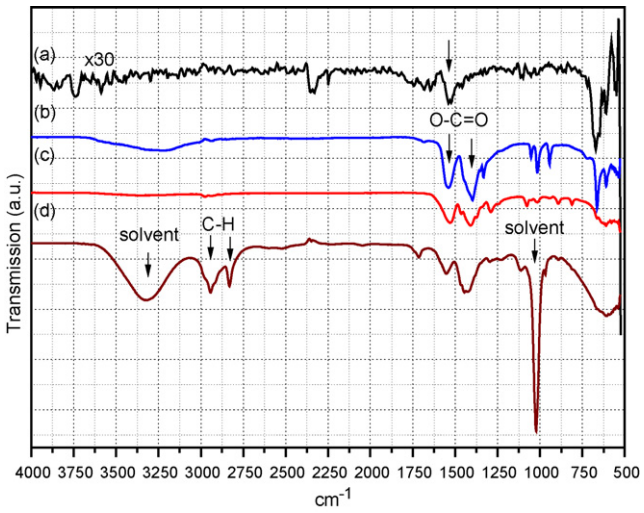

Fig. 9. FTIR spectra of a LZO film annealed at 900 °C for an hour (a). Curves b, c, and d show a lanthanum acetate hydrate, a LZO precursor film dried at 150 °C for an hour, and a precursor solution, respectively.

by heating. This process may be called as solution–gel rather than sol–gel [19].

3.5. Carboxylates in LZO during the annealing process

Fig. 8 presents weight loss of a drop of the LZO precursor solution and a piece of the LZO precursor film dried at room temperature. The TGA data exhibit that about 55% weight is eliminated from either the LZO precursor solution or the dried LZO film at about 400 °C, which is ascribed to the removal of organic compounds. The weight loss seems to have a transition between 250 and 300 °C, where the rate of weight loss is relatively slow before the transition. This is possibly due to stronger chemical interactions between molecules during the formation of gel. Note that after 400 °C the weights of both samples continuously decrease until as high as 900 °C. In general, pure organic materials will not survive at such a high temperature as their boiling temperatures are low. For example, boiling temperatures of CH_3COOH, C_2H_5COOH, C_3H_7OH, and CH_3OH used in this study are only 118.1, 140.7, 97.1, and 64.7 °C, respectively. So this phenomenon elucidates that the weight loss is from the compounding of LZO in the gel, where organic matters are gradually remove by thermal heating during the annealing process. The weight loss should not be caused by inorganic compounds, as boiling temperatures of ceramics are much higher than 900 °C, for example ZiO_2 > 2700 °C, La_2O_3 > 4100 °C, and LZO > 2000 °C.

Fig. 9 shows a FTIR spectrum of a LZO film annealed at 900 °C for an hour (curve a). It indicates that most of the organic-related peaks, for example, C–H stretch at 2826 and 2948 cm^{-1} are absent in the LZO film. Unexpectedly, absorptions in the ranges of 539–665 and 1403–1541 cm^{-1} caused by O–C=O of carboxylates are still present. Moreover, when the film is irradiated by the electron beam for about three minutes at a high magnification in FEGSEM, a dark region appears on the LZO film (data not shown), which may be due to the organic compounds in the LZO film such as hydrocarbon [20]. The above results suggest that carboxylates related organic compounds reside in the LZO film during the annealing process. The role of the carboxylates has not been identified in this study. But it is believed that the carboxylates probably affect the compounding of La and Zr metal ions as the carboxylate ions–metal ions in the gel could have some interactions, and therefore influence the microstructure of LZO films. A study based on the statistics has suggested that the ratio of lanthanum acetate to propionic

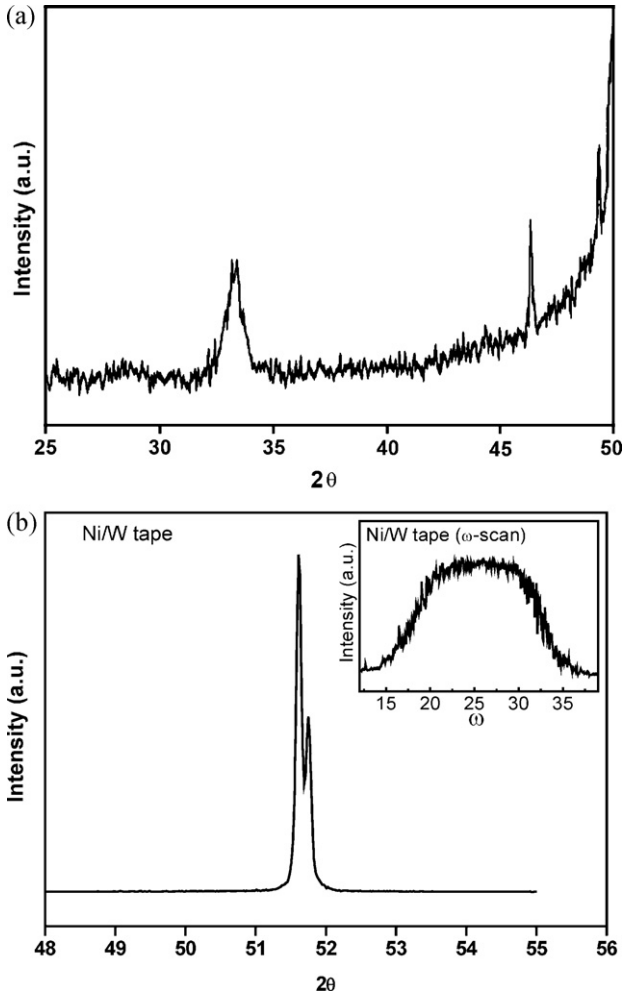

Fig. 10. (a) XRD pattern of a LZO film measured in the θ–2θ scan mode. (b) θ–2θ scan XRD pattern of a Ni-5%W substrate. The single peak at 51.6° indicates the substrate is textured. The inset is a corresponding spectrum in the ω-scan mode.

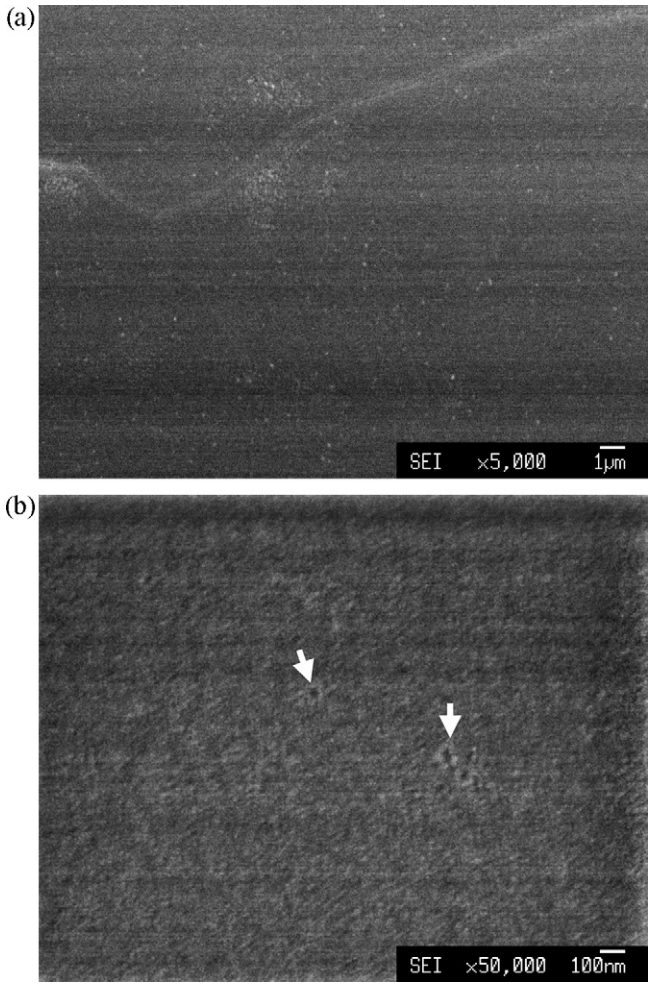

Fig. 11. FEGSEM of a LZO film imaged at 5000× (a) and 50,000× (b). The arrows indicate pin holes are present.

acid is a crucial factor for the out-of-plane texture of LZO films [21].

Fig. 10 gives XRD patterns of a LZO film coated by an inkjet printer on a Ni-5%W substrate annealed at 900 °C for an hour. It is known that LZO can grow epitaxially on textured Ni or Ni/W substrates [9–10]. As shown in Fig. 10a, the LZO film displays only a (4 0 0) peak, suggesting that the LZO lattice have a good alignment along ⟨4 0 0⟩ directions. Fig. 10b is the XRD data of the textured Ni/W substrate. FEGSEM images display that the LZO film surface is smooth and dense, as shown in Fig. 11a. Fig. 11b is imaged at a high magnification showing that the LZO film composed of small nanocrystals sizing about 10–15 nm. Some pinholes estimated about 25–35 nm in diameter are found to be less than 0.1% in the area. The effect of carboxylates on the surface morphology is not clear. But it was found that the ratio of lanthanum acetate to propionic acid has a comparable degree of importance to the annealing temperature [21].

3.6. Growth mechanism

Based on the above results, it is concluded that the growth of LZO films involves following stages. First, La and Zr solutions form a LZO precursor solution, where La and Zr ions are present in the form of stable organic–inorganic complex compounds. Second, removal of solvents and decomposition of zirconium propoxides, followed by formation of gel, happen in the early stage of annealing process. Finally, LZO compounds grow into a nanocrystalline film in the presence of carboxylates. The results enable us to identify experimental factors affecting the microstructure of LZO films more accurately and indicate that the chemistry of a precursor solution plays an important role in the wet chemical synthesis.

4. Conclusions

Pyrochlore lanthanum zirconium oxide thin films textured along ⟨4 0 0⟩ have been fabricated using lanthanum acetate hydrate, zirconium propoxide, propionic acid, acetic acid glacial, and methanol as precursors. Annealed LZO films composed of nanocrystallites sizing 10–15 nm have a dense and smooth structure and rare pinholes sizing 25–35 nm. The formation of the LZO films is based on the decomposition of a mixture of La and Zr solution. Zr metal–oxide bonds are found to be first eliminated at around 250 °C that leads to the formation of a gel. Subsequent annealing at 900 °C for an hour causes the compounding and the formation of LZO film in the presence of carboxylates. The process is identified as a solution–gel process.

References

[1] J.W. Seo, J. Fompeyrine, A. Guiller, G. Norga, C. Marchiori, H. Siegwart, J.P. Locquet, Appl. Phys. Lett. 83 (2003) 5211.
[2] S. Sathyamurthy, M. Paranthaman, H.Y. Zhai, H.M. Christen, P.M. Martin, A. Goyal, J. Mater. Res. 17 (2002) 1543.
[3] S. Engel, K. Knoth, R. Huhne, L. Schultz, B. Holzapfel, Supercond. Sci. Technol. 18 (2005) 13851390.
[4] F.W. Poulsen, N. Puil, Solid State Ionics 777 (1994) 53.
[5] G. Chiodelli, M. Scagliotti, Solid State Ionics 73 (1994) 265.
[6] H. Kido, S. Komarneni, R. Roy, J. Am. Ceram. Soc. 74 (1991) 422.
[7] J. Nair, P. Nair, G.B.M. Doesburg, J.G. Ommen, J.R.H. Ross, A.J. Burggraaf, F. Mizukami, J. Am. Ceram. Soc. 82 (1999) 2066.
[8] T.G. Chirayil, M. Paranthaman, D.B. Beach, D.F. Lee, A. Goyal, R.K. William, X. Cui, D.M. Kroeger, R. Feenstra, D.T. Verebelyi, D.K. Christen, Physica C 336 (2000) 63.
[9] S. Sathyamurthy, M. Paranthaman, H.Y. Zhai, H.M. Christen, P.M. Martin, A. Goyal, J. Mater. Res. 17 (2002) 2181.
[10] K. Knoth, B. Schlobach, R. Huhne, L. Schultz, B. Holzapfel, Physica C 426–431 (2005) 979.
[11] J. Lian, L.M. Wang, R.G. Haire, K.B. Helean, R.C. Esing, Nucl. Instrum. Methods Phys. Res. B 218 (2004) 236.
[12] A. Ota, Y. Matsumura, M. Yoshinaka, K. Hirota, O. Yamaguchi, J. Mater. Sci. Lett. 17 (1998) 199.
[13] M.C. Cordero-Cabrera, T. Mouganie, B.A. Glowacki, M. Baecker, M. Falter, B. Holzapfel, J. Engell, J. Mater. Sci. 42 (2007) 7129.
[14] V.S. Sarma, J. Eickemeyer, L. Schultz, B. Holzapfel, Scripta Mater. 50 (2004) 953.
[15] T. Mouganie, B.A. Glowacki, J. Mater. Sci. 41 (2006) 8257.
[16] S.M.R. Rocha, C.A.S. Queiroz, A. Abrao, J. Alloys Compd. 344 (2002) 389.
[17] M. Nabavi, S. Doeuff, C. Sanchez, J. Livage, J. Non-Cryst. Solid 121 (1990) 31.
[18] C.J. Brinker, G.W. Scherer, Sol–Gel Science: The Physics and Chemistry of Sol–Gel Processing, Academic Press, London, 1990.
[19] J. Livage, C. Sanchez, M. Henry, S. Doeuff, Solid State Ionics 32/33 (1989) 633.
[20] N. Morita, N. Kawasegi, K. Ooi, Nanotechnology 19 (2008) 155302.
[21] H.S. Chen, R.V. Kumar, B.A. Glowacki, J. Sol–Gel Sci. Technol. 51 (2009) 102.